Appendix A

Supplementary data

for

The state of platinum in pyrrhotite: X-ray absorption spectroscopy study and implications for the role of Fe sulfides as platinum carriers

Olga N. Filimonova, Alexander L. Trigub, Maximilian S. Nickolsky, Dmitriy A. Chareev, Kristina O. Kvashnina, Elena V. Kovalchuk, Ilya V. Vikentyev, Vladimir L. Reukov, and Boris R. Tagirov*

Mineralogical Magazine

***Corresponding author**: Institute of Geology of Ore Deposits, Petrography, Mineralogy and Geochemistry (IGEM RAS), 35, Staromonetnyi per., 119017 Moscow, Russia; *e-mail* boris1t@yandex.ru

Table A.1. The operating conditions of EPMA.

EPMA conditions	**Pt**	**Fe**	**S**
Crystal analyser	PETH	LIF	PETH
Analytical line	PtMα	Kα	Kα
Accelerating voltage	20 kV		
Current in the Faraday cup	20 nA		
Exposure	30 s	20 s	10 s
Probe diameter	1 μm		
Detection limit (2σ)	600 ppm	270 ppm	130 ppm

Table A.2. The operating conditions of LA-ICP-MS.

LA-ICP-MS conditions	
RF power	1350 W
Plasma gas	14.2 L min^{-1} Ar
Auxiliary gas	0.7 L min^{-1} Ar
Make-up gas	0.8 L min^{-1} Ar
Sampling depth	1.5 mm
Detector	Dual (pulse and analogue counting)
Dwell time/mass	10 ms
Laser parameters	
Wavelength	213 nm
Energy density	4-7 J cm^{-2}
Carrier gas	0.6 He
Ablation style	Single spot/ line
Ablation spot size	60/40 μm
Repetition rate	10 Hz

Table A.3. Composition of Pt-bearing pyrite and pyrrhotite measured by EPMA and LA-ICP-MS.

WDS Sample (Point) id	Fe, wt.%	S, wt.%	Pt, wt.%	Fe, at.%	S, at.%	Pt, at.%
Synthesis temperature *t* = 720 °C						
pyrrhotite, 5602 (1)	59.74	38.97	0.57	46.75	53.12	0.13
pyrrhotite, 5602 (2)	59.60	39.13	0.60	46.59	53.28	0.13
pyrrhotite, 5602 (3)	59.35	39.17	0.58	46.46	53.41	0.13
pyrrhotite, 5602 (4)	59.44	39.25	0.61	46.45	53.42	0.14
pyrrhotite, 5602 (5)	59.44	39.37	0.59	46.37	53.50	0.13
pyrrhotite, 5602 (6)	59.14	38.92	0.58	46.53	53.34	0.13
pyrrhotite, 5602 (7)	59.83	39.06	0.53	46.74	53.14	0.12
pyrrhotite, 5602 (8)	59.96	38.87	0.47	46.92	52.98	0.11
pyrrhotite, 5602 (9)	60.12	38.84	0.36	47.02	52.90	0.08
Average content	**59.6**	**39.1**	**0.5**	**46.7**	**53.2**	**0.12**
±2SD	**0.6**	**0.4**	**0.2**	**0.4**	**0.4**	**0.04**
Synthesis temperature *t* = 650 °C						
pyrrhotite, 5601 (1)	59.87	38.58	0.34	47.08	52.84	0.08
pyrrhotite, 5601 (2)	60.54	38.57	0.31	47.37	52.56	0.07
pyrrhotite, 5601 (3)	60.05	38.65	0.33	47.11	52.81	0.07
pyrrhotite, 5601 (4)	60.19	38.68	0.31	47.15	52.78	0.07
pyrrhotite, 5601 (5)	60.13	38.82	0.30	47.04	52.89	0.07
pyrrhotite, 5601 (6)	60.03	38.67	0.30	47.09	52.84	0.07
pyrrhotite, 5601 (7)	60.62	39.12	0.07	47.07	52.91	0.02
Average content	**60.2**	**38.7**	**0.3**	**47.1**	**52.8**	**0.06**
±2SD	**0.6**	**0.4**	**0.2**	**0.2**	**0.2**	**0.04**
pyrite, 5601 (1)	46.45	52.13	0.19	33.83	66.13	0.04
pyrite, 5601 (2)	45.95	52.23	1.00	33.49	66.30	0.21
pyrite, 5601 (3)	46.08	51.73	0.29	33.82	66.12	0.06
pyrite, 5601 (4)	45.75	51.46	1.01	33.72	66.06	0.21
Average content	**46.1**	**51.9**	**0.6**	**33.7**	**66.2**	**0.13**
±2SD	**0.6**	**0.7**	**0.9**	**0.4**	**0.9**	**0.19**
pyrrhotite, 5599 (1)	61.46	37.13	0.017[A]	48.73	51.27	0.004
pyrrhotite, 5599 (2)	61.65	37.23	0.017[A]	48.74	51.26	0.004
pyrrhotite, 5599 (3)	61.41	37.22	0.017[A]	48.64	51.35	0.004
pyrrhotite, 5599 (4)	62.05	37.34	0.017[A]	48.82	51.17	0.004
pyrrhotite, 5599 (5)	61.43	37.11	0.017[A]	48.73	51.27	0.004
pyrrhotite, 5599 (6)	61.74	37.09	0.017[A]	48.87	51.13	0.004
Average content	**61.6**	**37.2**	**0.02**[A]	**48.8**	**51.2**	**0.004**
±2SD	**0.5**	**0.2**	**<0.01**[A]	**0.2**	**0.2**	**<0.001**
pyrrhotite, 5592 (1)	60.17	38.73	0.32	47.11	52.82	0.07
pyrrhotite, 5592 (2)	60.09	38.9	0.36	46.97	52.95	0.08
pyrrhotite, 5592 (3)	59.78	38.63	0.31	47.01	52.92	0.07
pyrrhotite, 5592 (4)	59.89	38.86	0.28	46.92	53.02	0.06
pyrrhotite, 5592 (5)	59.99	38.89	0.28	46.94	53.00	0.06
pyrrhotite, 5592 (6)	60.19	38.67	0.11	47.18	52.79	0.02
Average content	**60.0**	**38.8**	**0.3**	**47.0**	**52.9**	**0.06**
±2SD	**0.3**	**0.2**	**0.2**	**0.2**	**0.2**	**0.04**

Table A.3. – continued.

WDS Sample (Point) id	Fe, wt.%	S, wt.%	Pt, wt.%	Fe, at.%	S, at.%	Pt, at.%
pyrite, 5592 (1)	43.33	51.67	1.59	32.39	67.27	0.34
pyrite, 5592 (2)	46.36	51.90	0.45	33.87	66.04	0.09
pyrite, 5592 (3)	45.19	51.39	0.61	33.51	66.36	0.13
pyrite, 5592 (4)	45.94	51.93	0.39	33.66	66.26	0.08
pyrite, 5592 (5)	45.32	51.78	2.47	33.27	66.21	0.52
pyrite, 5592 (6)	46.42	52.14	0.17	33.81	66.15	0.04
Average content	**45.4**	**51.8**	**1.0**	**33.4**	**66.4**	**0.20**
±2SD	**2.3**	**0.5**	**1.8**	**1.7**	**0.7**	**0.38**
pyrrhotite, 5590 (1)	60.09	38.72	0.31	47.09	52.84	0.07
pyrrhotite,5590 (2)	59.22	38.67	0.38	46.75	53.17	0.09
pyrrhotite,5590 (3)	59.78	38.78	0.37	46.91	53.00	0.08
pyrrhotite,5590 (4)	59.83	38.78	0.38	46.93	52.98	0.09
pyrrhotite,5590 (5)	59.65	38.71	0.32	46.91	53.02	0.07
pyrrhotite,5590 (6)	59.45	38.5	0.37	46.95	52.96	0.08
pyrrhotite,5590 (7)	59.88	38.57	0.37	47.09	52.83	0.08
Average content	**59.7**	**38.7**	**0.4**	**47.0**	**53.0**	**0.08**
±2SD	**0.6**	**0.2**	**0.1**	**0.2**	**0.2**	**0.02**
pyrite, 5590 (1)	45.88	52.96	0.40	33.19	66.73	0.08
pyrite, 5590 (2)	45.05	51.99	2.12	33.07	66.48	0.45
pyrite, 5590 (3)	46.03	52.09	0.33	33.64	66.30	0.07
pyrite, 5590 (4)	45.65	52.16	1.67	33.33	66.32	0.35
pyrite, 5590 (5)	45.63	52.22	1.02	33.34	66.45	0.21
pyrite, 5590 (6)	44.97	51.60	1.88	33.22	66.39	0.40
Average content	**45.5**	**52.2**	**1.2**	**33.3**	**66.4**	**0.26**
±2SD	**0.9**	**0.9**	**1.5**	**0.6**	**1.1**	**0.32**

[A] determined via LA-ICP-MS analysis

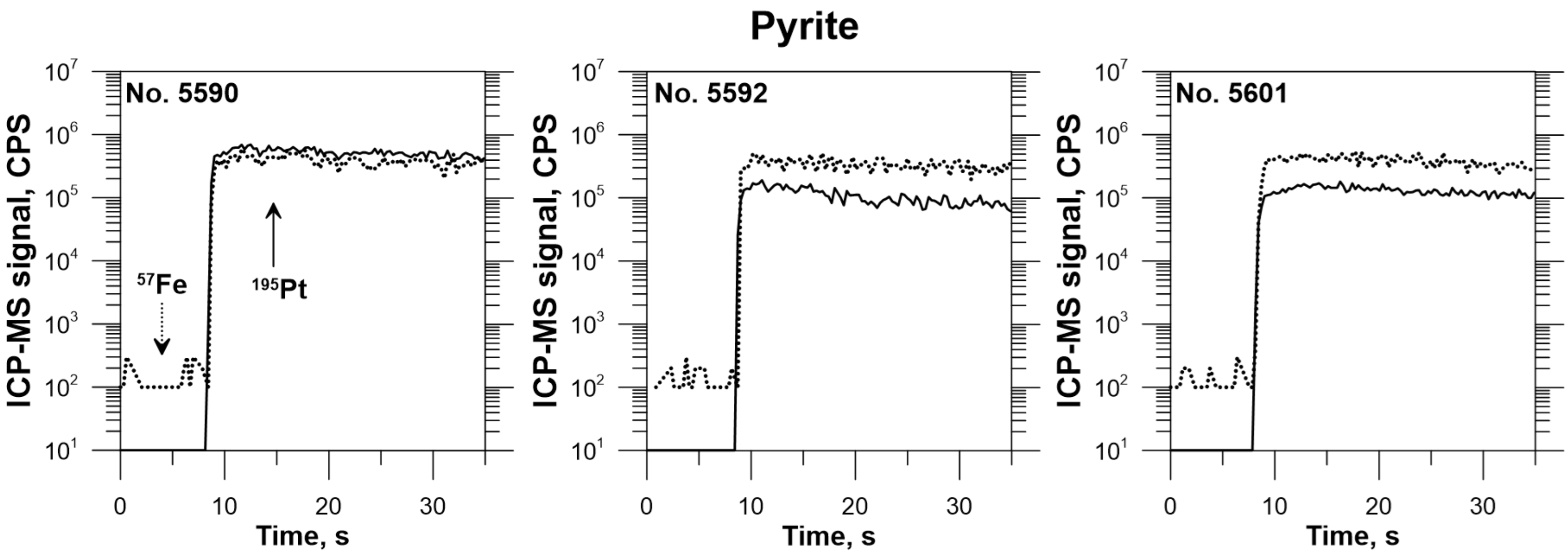

Figure A.1. Time-resolved laser ablation ICP-MS spectra of Pt-bearing synthetic pyrites. Analyses were performed using a spot size of 60 μm. The ^{195}Pt (solid lines) disseminated in the pyrite matrix behaves similarly to the internal standard element – ^{57}Fe (dotted lines).

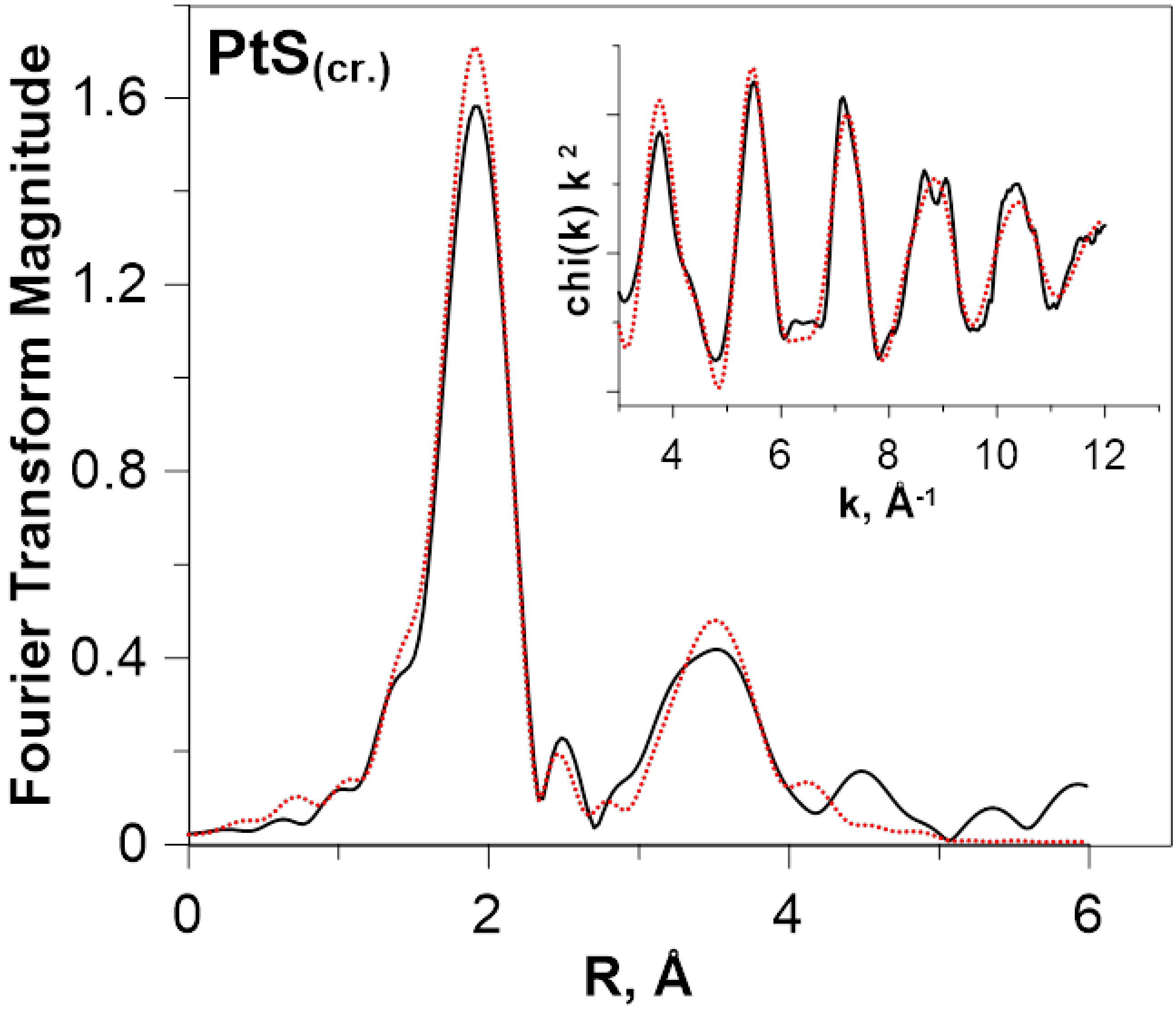

Figure A.2. The Pt L_3-edge EXAFS spectrum of $PtS_{(cr)}$ and fit results: Fourier Transform (FT) of the k^2-weighted EXAFS spectrum (not corrected for phase shift), ***insert:*** k^2-weighted background-subtracted EXAFS spectrum. Thin black line – experiment, dotted red line – fit results. The 1st coordination sphere of Pt consists of 4 S at $R_{Pt\text{-}S}$ = 2.31±0.01 Å, the 2nd coordination sphere consists of 4 and 8 Pt atoms at $R_{Pt\text{-}Pt}$ = 3.49±0.05 and 3.87±0.07 Å, respectively, the 3rd coordination sphere consists of 8 S atoms at $R_{Pt\text{-}S}$ = 4.09±0.03 Å.

No. 5602

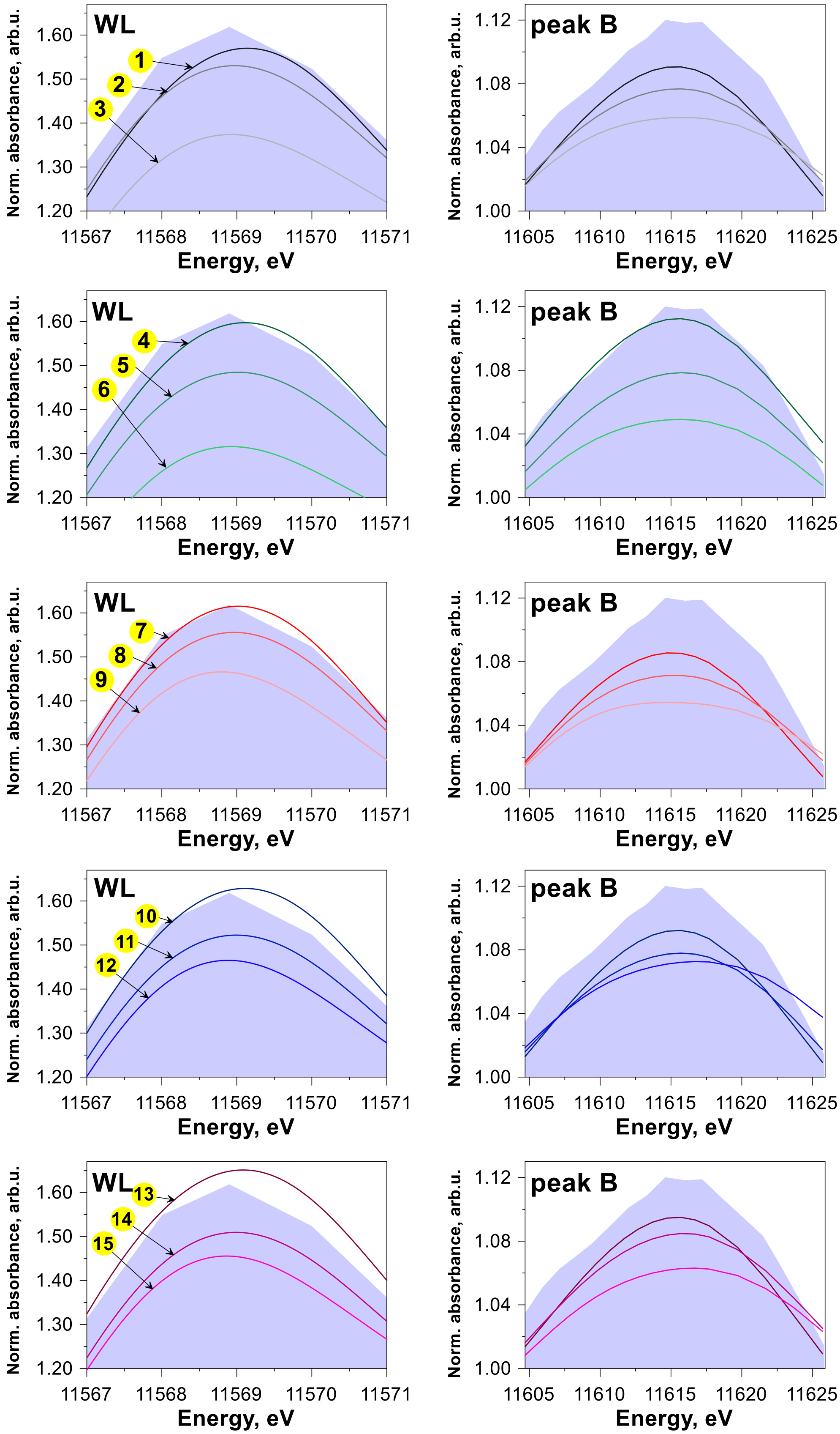
WL
peak B
1
2
3
4
5
6
7
8
9
10
11
12
13
14
15
Norm. absorbance, arb.u.
Energy, eV
1.20
1.30
1.40
1.50
1.60
11567
11568
11569
11570
11571
1.00
1.04
1.08
1.12
11605
11610
11615
11620
11625

No. 5601

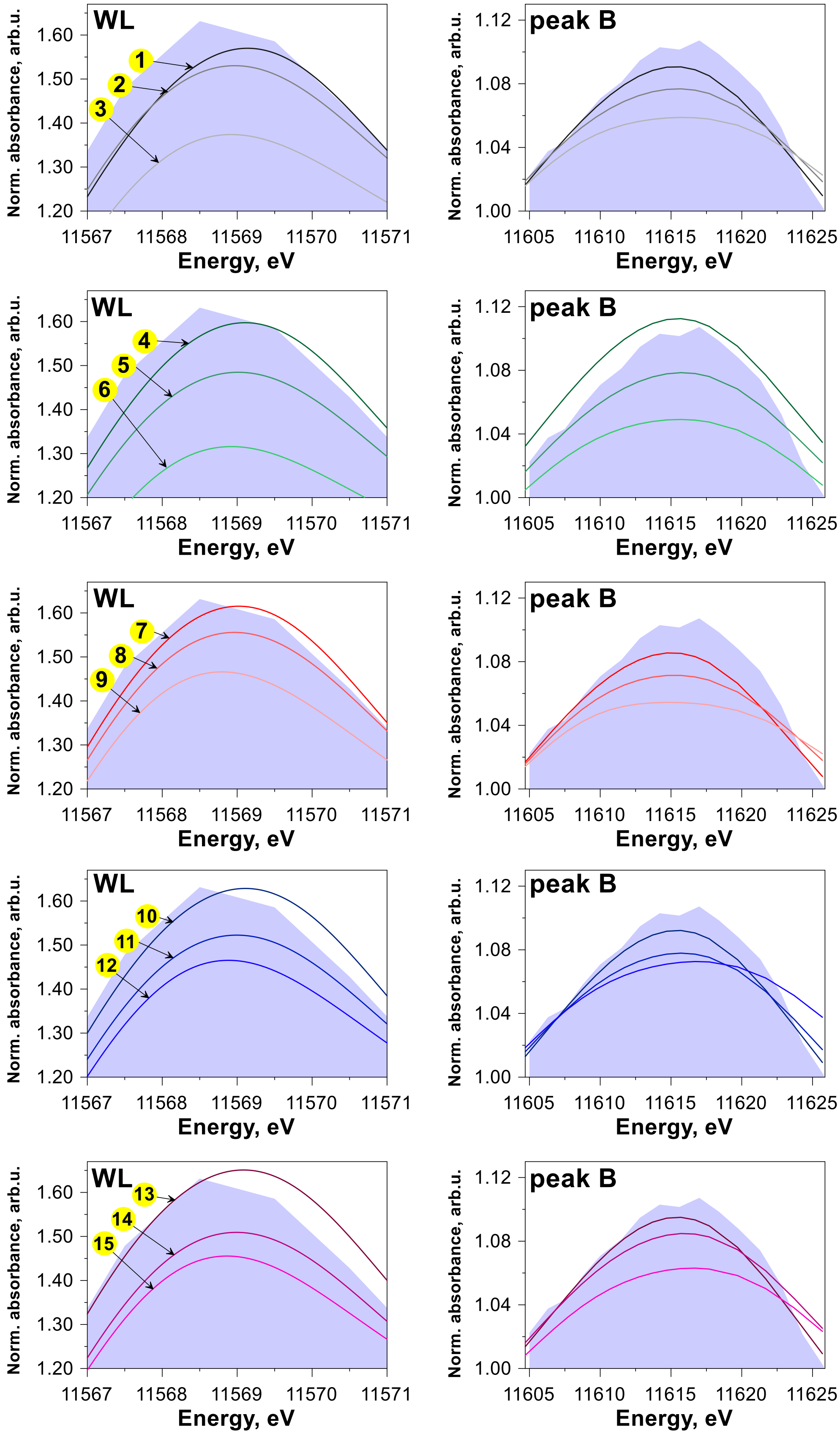

WL
peak B
Norm. absorbance, arb.u.
Energy, eV
1
2
3
4
5
6
7
8
9
10
11
12
13
14
15

No. 5599

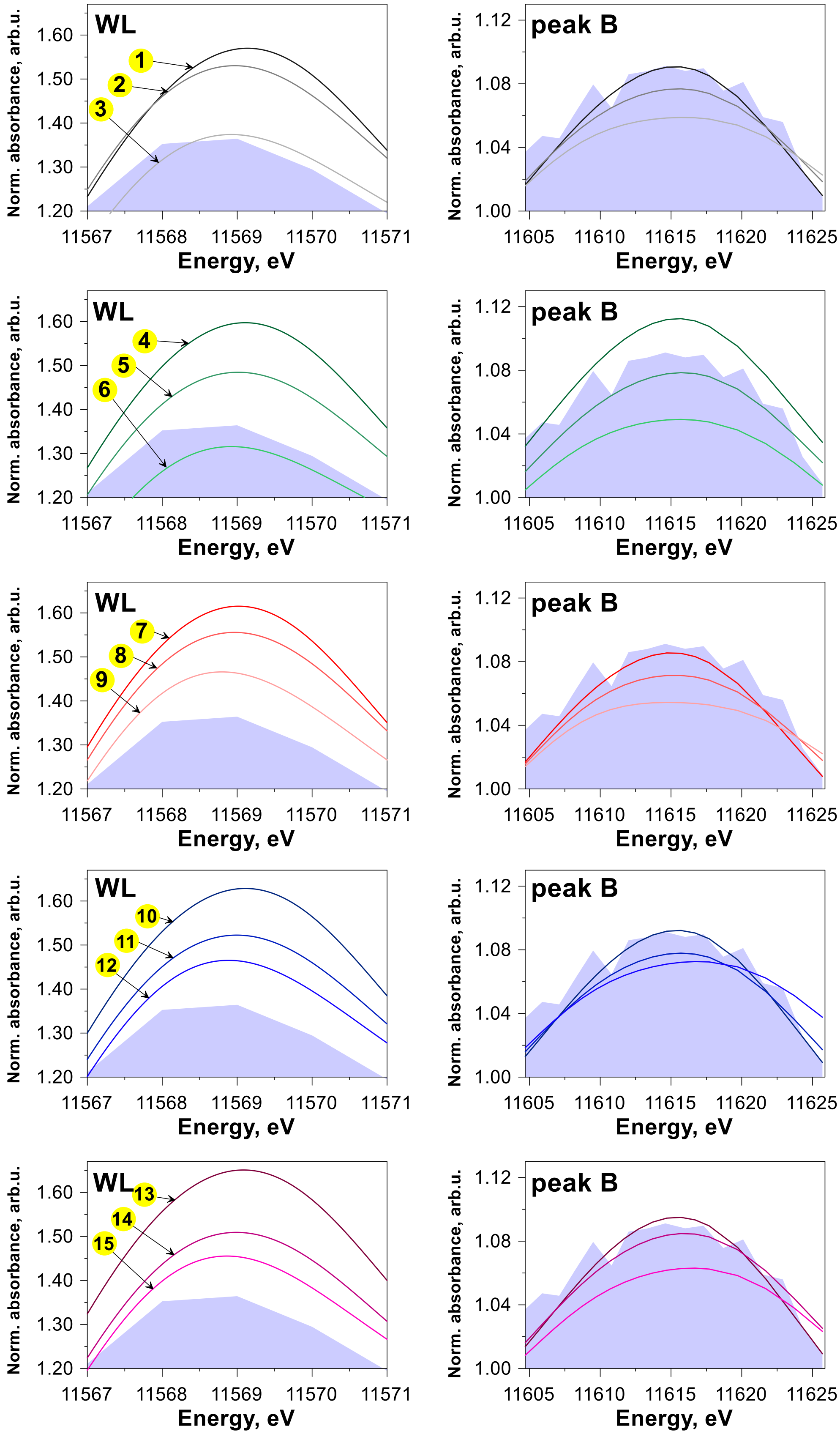

WL
peak B
Norm. absorbance, arb.u.
Energy, eV
1.60
1.50
1.40
1.30
1.20
1.12
1.08
1.04
1.00
11567
11568
11569
11570
11571
11605
11610
11615
11620
11625
1
2
3
4
5
6
7
8
9
10
11
12
13
14
15

No. 5592

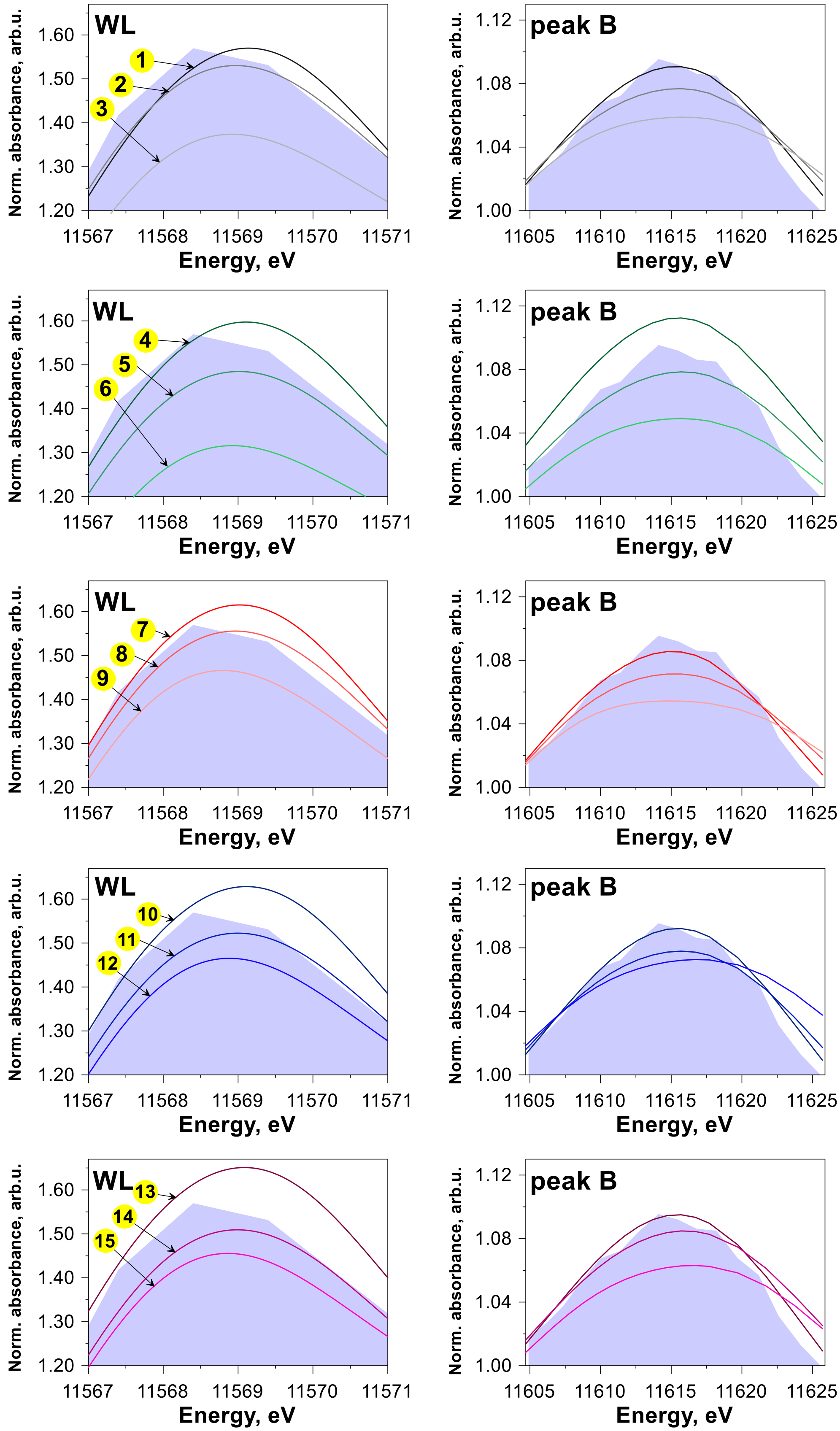
WL
peak B
1
2
3
4
5
6
7
8
9
10
11
12
13
14
15
Norm. absorbance, arb.u.
Energy, eV
1.20
1.30
1.40
1.50
1.60
1.00
1.04
1.08
1.12
11567
11568
11569
11570
11571
11605
11610
11615
11620
11625

No. 5590

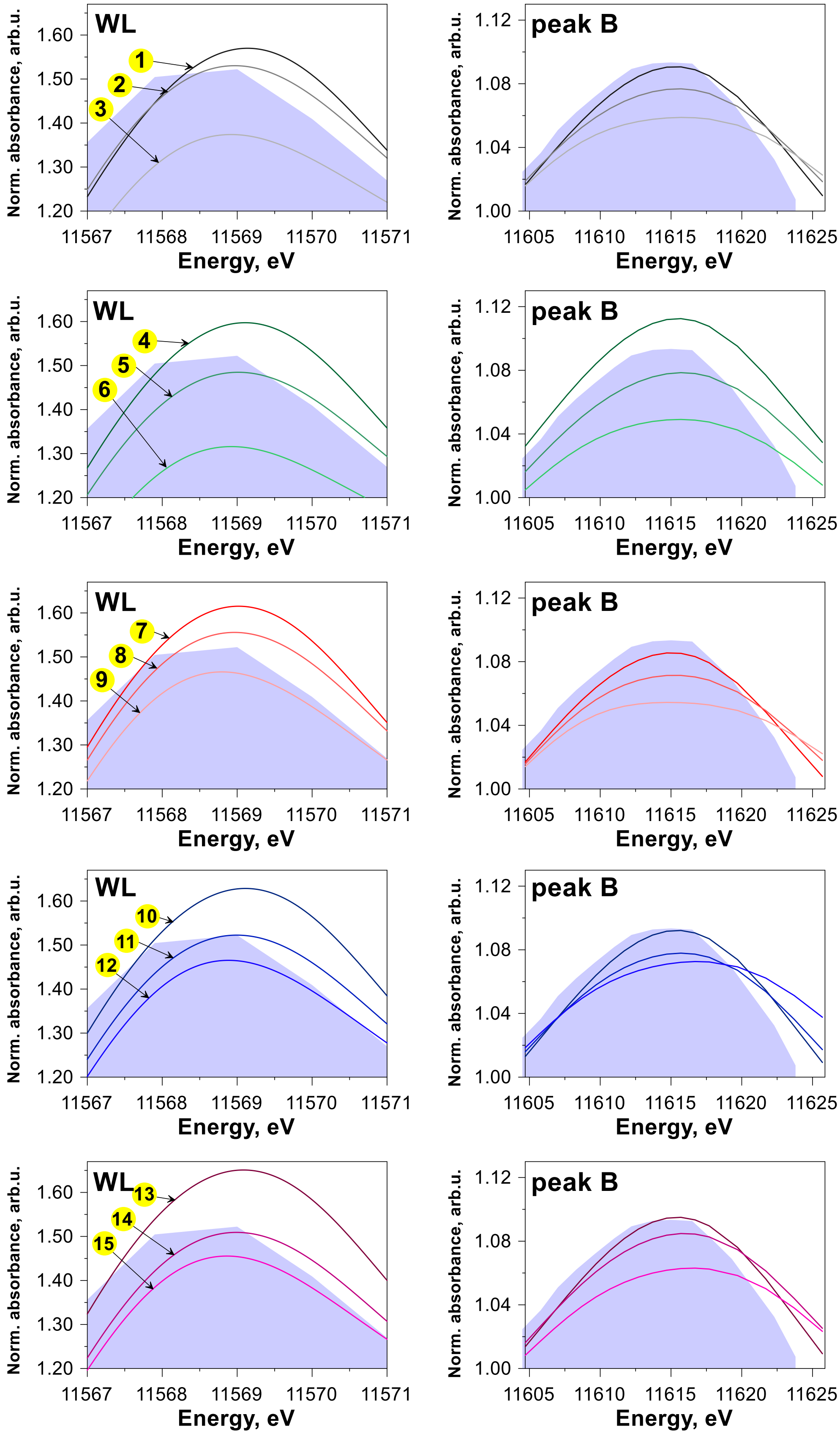
WL
peak B
Norm. absorbance, arb.u.
Energy, eV
1.20
1.30
1.40
1.50
1.60
1.00
1.04
1.08
1.12
11567
11568
11569
11570
11571
11605
11610
11615
11620
11625
1
2
3
4
5
6
7
8
9
10
11
12
13
14
15

Figure A.3. Enlarged portions of Pt L_3-edge XANES spectra of pyrrhotite samples: WL (*left*) and peak B (*right*) regions. The experimental spectra are shown by blue fields, the spectra calculated by FDMNES code are shown by solid lines. The number of S atoms in the 1st coordination shell varied from 6 to 4, the number of Fe atoms in the 2nd coordination shell varied from 5 to 8. Each model spectrum was calculated for various numbers of S and Fe atoms in the 1st and 2nd coordination shells. The distant coordination shells correspond to a pure pyrrhotite structure adopted from Wyckoff (1963). The sequence number of the model is indicated in the yellow circle in every picture and explained below:

(1) 6 S, 8 Fe,
(2) 5 S, 8 Fe,
(3) 4 S, 8 Fe,
(4) 6 S, 7 Fe (one vacancy in the Fe site at $R_{Pt\text{-}Fe}$ = 3.43 Å),
(5) 5 S, 7 Fe (one vacancy in the Fe site at $R_{Pt\text{-}Fe}$ = 3.43 Å),
(6) 4 S, 7 Fe (one vacancy in the Fe site at $R_{Pt\text{-}Fe}$ = 3.43 Å),
(7) 6 S, 7 Fe (one vacancy in the Fe site at $R_{Pt\text{-}Fe}$ = 2.84 Å),
(8) 5 S, 7 Fe (one vacancy in the Fe site at $R_{Pt\text{-}Fe}$ = 2.84 Å),
(9) 4 S, 7 Fe (one vacancy in the Fe site at $R_{Pt\text{-}Fe}$ = 2.84 Å),
(10) 6 S, 6 Fe (two vacancies in Fe sites at $R_{Pt\text{-}Fe}$ = 3.43 Å: atoms Nos. 1, 2 in Fig. 7),
(11) 5 S, 6 Fe (two vacancies in the Fe sites at $R_{Pt\text{-}Fe}$ = 3.43 Å: atoms Nos. 1, 2 in Fig. 7),
(12) 4 S, 6 Fe (two vacancies in the Fe sites at $R_{Pt\text{-}Fe}$ = 3.43 Å: atoms Nos. 1, 2 in Fig. 7),
(13) 6 S, 5 Fe (three vacancies in the Fe sites at $R_{Pt\text{-}Fe}$ = 3.43 Å: atoms Nos. 1, 4, 5 in Fig. 7),
(14) 5 S, 5 Fe (three vacancies in the Fe sites at $R_{Pt\text{-}Fe}$ = 3.43 Å: atoms Nos. 1, 4, 5 in Fig. 7),
(15) 4 S, 5 Fe (three vacancies in the Fe sites at $R_{Pt\text{-}Fe}$ = 3.43 Å: atoms Nos. 1, 4, 5 in Fig. 7).